Theoretical Studies of Bridging-Ligand Effects in Quadruply Bonded Dichromium(II) Compounds. 3. The First Complete Geometry Optimizations of Transition-Metal Dimer Complexes

Randall D. Davy and Michael B. Hall*

Contribution from the Department of Chemistry, Texas A&M University, College Station, Texas 77843. *Received May 17, 1988*

Abstract: Generalized valence bond (GVB) calculations are reported for a series of dichromium(II) complexes. Analytical gradient techniques were used to completely optimize the geometries of $Cr_2(O_2CH)_4$, $Cr_2((NH)OCH)_4$, and $Cr_2((NH)_2CH)_4$ as well as partially optimize the geometries of $Cr_2(O_2CH)_4(H_2O)_2$ and $Cr_2((NH)_2CH)_4(H_2O)_2$ at the GVB level. The geometry of the bridging ligand strongly affects the calculated Cr–Cr bond length; thus, complete geometry optimizations are necessary for dichromium complexes with different bridging ligands. Even with complete optimization, the Cr–Cr bond is calculated to be too long at the GVB level, but the calculated trends in Cr–Cr bond lengths are more accurate. The calculated changes in Cr–Cr bond length are 0.08 and 0.11 Å for the bridging ligand changes formato to amidato and amidato to amidinato, respectively. Upon axial hydration, the Cr–Cr bond is calculated to lengthen by 0.11 Å for $Cr_2(O_2CH)_4$ and 0.18 Å for $Cr_2((NH)_2CH)_4$. Again, calculations underestimate the effect of axial ligands on Cr–Cr bond length, but the trends in Cr–Cr bond lengths for the axially ligated complexes as well as the *relative* response to axial ligands are consistent with experimental results. Our calculated trends in Cr–Cr bond length are consistent with a Cr–Cr bond length of 2.05–2.10 Å for dichromium tetracarboxylates without axial ligands.

Quadruply bonded complexes of dichromium(II) have been the subject of on-going theoretical[1-17] and experimental[18-30] studies. These complexes are interesting for the wide range of lengths exhibited by formally quadruple bonds between chromium atoms. Most studies have focused on complexes with the general formula $Cr_2(bridge)_4L_n$ with $n = 0$, 1, or 2 (see Figure 1). Although the Cr–Cr bond lengths are wide ranging, the complexes generally fall into two distinct classes. The largest class is characterized by bridging ligands derived from carboxylates and the presence of axial ligands. These complexes have Cr–Cr bond lengths in the range 2.28 to 2.54 Å. The second class, with super-short Cr–Cr bonds, is characterized by bridging ligands derived from acids weaker than carboxylic and the absence of axial ligands.

Studies on these complexes have tried to divide the responsibility for the change in Cr–Cr bond length between the two changes in ligation, and a controversy has arisen between theory and experiment in this effort. There are two obvious experimental approaches to determining the cause of the bond length change. One may either add axial ligands to the complexes with super-short bonds or remove the axial ligands from the complexes with long bonds. Cotton and co-workers showed that the Cr–Cr bond of the complex $Cr_2(O(NR)CMe)_4$ (R = 2-xylyl) can be lengthened from 1.937 (2) to 2.354 (5) Å by the addition of axial ligands.[25,26] This would suggest that the principal difference between the classes is the presence of axial ligands. Therefore, one would also postulate that the removal of axial ligands from the tetracarboxylate complexes should substantially shorten the Cr–Cr bond. Initial efforts to test this postulate were frustrated by the difficulty of crystallizing a tetracarboxylate complex that lacked any form of axial ligation. The postulate was tested by calculations, and they indicated that the Cr–Cr bond remains long and weak in the absence of axial ligands.[9,16] Thus the shortening of Cr–Cr bond postulated from the experiments was not found by theory.

The controversy concerning the relative effects of axial and bridging ligation has been difficult to resolve because of difficulties in both experiments and calculations. Crystallization of tetracarboxylate complexes without axial ligation has not yet been accomplished, despite great effort.[27] Since the complete removal of axial ligands is so difficult, Cotton and Wang[19] plotted the change in Cr–Cr bond length as a function of axial and bridging ligand pK_a for a series of tetracarboxylate complexes. They found that the Cr–Cr bond length for these complexes are more sensitive to the pK_a of the bridging ligand (ΔCr–Cr is approximately −0.04 Å/pK_a unit) than the axial ligand (ΔCr–Cr is approximately 0.008 Å/pK_a unit). Although these plots cannot be extrapolated to the complete absence of axial ligands, they do show that the bridging ligand strongly affects the Cr–Cr bond length in complexes that have relatively long and weak metal-metal bonds. Recently the complex $Cr_2(O_2CCPh_3)(C_6H_6)_2$ has been prepared and characterized.[28] The benzene molecules are centered axially between two Cr–Cr units, with the benzene plane perpendicular to the

---

(1) Hall, M. B. *Polyhedron* **1987**, *6*, 679.
(2) Hall, M. B. In *Quantum Chemistry: The Challenge of Transition Metals and Coordination Chemistry*; Veillard, A., Ed.; D. Reidel: Amsterdam, 1986.
(3) Part 2: Kok, R. A.; Hall, M. B. *Inorg. Chem.* **1985**, *24*, 1542.
(4) Part 1: Kok, R. A.; Hall, M. B. *J. Am. Chem. Soc.* **1983**, *105*, 676.
(5) Wiest, R.; Benard, M. *Chem. Phys. Lett.* **1985**, *122*, 447.
(6) Weist, R.; Benard, M. *Chem. Phys. Lett.* **1983**, *98*, 102.
(7) Benard, M.; Coppens, P.; DeLucia, M. L.; Stevens, E. D. *Inorg. Chem.* **1980**, *19*, 1924.
(8) Benard, M. *J. Chem. Phys.* **1979**, *71*, 2546.
(9) Benard, M. *J. Am. Chem. Soc.* **1978**, *100*, 2354.
(10) Ziegler, T.; Tschinke, V.; Becke, A. *Polyhedron* **1987**, *6*, 685.
(11) Ziegler, T. *J. Am. Chem. Soc.* **1985**, *107*, 4453.
(12) Atha, P. M.; Campbell, J. C.; Garner, C. D.; Hillier, I. H.; MacDowell, A. A. *J. Chem. Soc., Dalton Trans.* **1983**, 1085.
(13) Atha, P. M.; Hillier, I. H.; Guest, M. F. *Mol. Phys.* **1982**, *46*, 437.
(14) Garner, C. D.; Hillier, I. H.; Knight, M. J.; MacDowell, A. A.; Walton, I. B.; Guest, M. F. *J. Chem. Soc., Faraday Trans. 2* **1980**, *76*, 885.
(15) Guest, M. F.; Garner, C. D.; Hillier, I. H.; Walton, I. B. *J. Chem. Soc., Faraday Trans. 2* **1978**, *74*, 2092.
(16) Guest, M. F.; Hillier, I. H.; Garner, C. D. *Chem. Phys. Lett.* **1977**, *48*, 587.
(17) Garner, C. D.; Hillier, I. H.; Guest, M. F.; Green, J. C.; Coleman, A. W. *Chem. Phys. Lett.* **1976**, *41*, 91.
(18) Cotton, F. A.; Walton, R. A. *Structure and Bonding* **1987**, *62*, 1085.
(19) Cotton, F. A.; Wang, W. *Nouv. J. Chim.* **1984**, *8*, 331.
(20) Cotton, F. A.; Walton, R. A. *Multiple Bonds between Metal Atoms*; Wiley: New York, 1982.
(21) Cotton, F. A.; Felthouse, T. R. *Inorg. Chem.* **1980**, *19*, 328.
(22) Cotton, F. A.; Rice, G. W. *Inorg. Chem.* **1978**, *17*, 2004.
(23) Cotton, F. A.; Extine, M. W.; Rice, G. W. *Inorg. Chem.* **1978**, *17*, 176.
(24) Cotton, F. A.; DeBoer, B. G.; LaPrade, M. D.; Pipal, J. R.; Ucko, D. A. *Acta Crystallogr.* **1971**, *B27*, 1664.
(25) Cotton, F. A.; Ilsley, W. H.; Kaim, W. *J. Am. Chem. Soc.* **1980**, *102*, 3464.
(26) Baral, S.; Cotton, F. A.; Ilsley, W. H. *Inorg. Chem.* **1981**, *20*, 2696.
(27) Cotton, F. A.; Thompson, J. L. *Inorg. Chem.* **1981**, *20*, 1292.
(28) Cotton, F. A. *J. Am. Chem. Soc.*, in press.
(29) Kektar, S. N.; Fink, M. *J. Am. Chem. Soc.* **1985**, *107*, 338.
(30) Garner, C. D.; Hillier, I. H.; MacDowell, A. A.; Walton, I. B.; Guest, M. F. *J. Chem. Soc., Faraday Trans. 2* **1979**, *75*, 485.

0002-7863/89/1511-1268$01.50/0

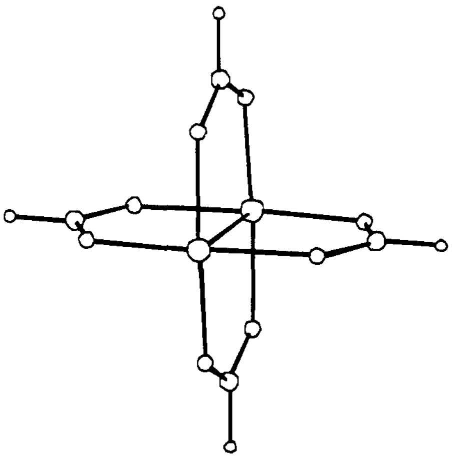

Figure 1. Dichromium tetraformate without axial ligands. Note the 4-fold symmetry axis typical of the complexes $Cr_2(bridge)_4$.

Cr–Cr axes, and the Cr to benzene-center distance of 3.30 Å. With this relatively weak axial interaction, the Cr–Cr bond is 2.256 (4) Å, which is the shortest seen in a crystalline complex of the type $Cr_2(O_2CR)_4L_n$. This bond length is still, however, much larger than the super-short Cr–Cr bonds (<2.0 Å).

To completely avoid the influence of axial ligands, gas-phase experiments have been performed on $Cr_2(O_2CMe)_4$. Kektar and Fink[29] found a Cr–Cr distance of 1.966 (14) Å by using gas-phase electron diffraction. Again, this would indicate that the axial ligands are responsible for the greater part of the bond distance change. The interpretation of this experiment was made difficult by the overlap of the radial distribution peaks for Cr–Cr and Cr–O and a low index of resolution. The gas-phase ultraviolet photoelectron spectrum (UV-PES) of $Cr_2(O_2CMe)_4$ has also been reported.[17] This spectrum differed substantially from the spectra of complexes with super-short Cr–Cr bonds, and the authors explained these differences by postulating a Cr–Cr bond which is outside the super-short range. The gas-phase spectrum of $Cr_2(O_2CMe)_4$ was compared to the spectrum in the solid state.[30] It is assumed that the dichromium tetraacetate is arranged in the solid state so that a bridging acetate ligand serves as the axial ligand to the neighboring complex. The peaks assigned to ionizations from the metal–metal bond are at lower energy in the solid-state spectrum, indicating a weakened bond. This experiment does not give a quantitative correlation between the absence of axial ligands and bond length, however. The experimental picture will perhaps not be complete until a crystal structure of a tetracarboxylate without axial ligation is obtained.

In a theoretical study one can make systematic changes which might be experimentally impossible. Computational studies of these complexes, however, have been difficult due to both the size of the system and the necessity of electron correlation in describing the Cr–Cr bond. The theoretical difficulties in calculations on metal–metal multiple bonds have been studied thoroughly[5,8] and reviewed recently by Hall.[1] We will discuss them briefly. The lack of electron correlation in the earliest calculations led to the incorrect conclusion that no bond existed between the chromium atoms; the ground state calculated at the restricted Hartee–Fock (RHF) approximation is $\sigma^2\pi^2\sigma^{*2}\pi^{*2}$.[17] In configuration interaction (CI) calculations the leading configuration is indeed the quadruply bonded one ($\sigma^2\pi^4\delta^2$). However, in calculations on $Cr_2(O_2CH)_4$ at Cr–Cr distances in the 2.25–2.50 Å range, the quadruply bonded configuration makes up less than 20% of the wave function.[9,3] The small contribution of the leading configuration indicates that a much larger CI calculation is required for the dichromium complexes than for a "typical" molecule, in which the leading configuration is 80% or more of the wave function. Thus, even when electron correlation is taken into account, ab initio calculations of Cr–Cr bond lengths in both the bare metal dimer[31,32] and in complexes do not in general provide correct absolute values. Walch et al.[33] estimate that 57 million configurations would be necessary to calculate a bond energy of even 0.6 eV for Cr_2, versus an experimental value of 2.0 eV.[34]

Although correct absolute values are difficult to calculate, one would expect CI calculations to reproduce experimental trends in bond lengths among dichromium tetracarboxylates and their derivatives. This has not been the case, however, if one accepts the Cr–Cr bond length of 1.966 Å determined by electron diffraction for $Cr_2(O_2CMe)_4$. Calculations by Kok and Hall[3] using CI on orbitals generated by the generalized molecular orbital method showed a difference of 0.48 Å between the Cr–Cr bond lengths of $Cr_2((NH)_2CH)_4$ and $Cr_2(O_2CH)_4$. The experimental difference for the complexes $Cr_2((NMe)_2CPh)_4$ and $Cr_2(O_2CMe)_4$ is only 0.13 Å. Benard calculated a change of only 0.05 Å upon addition of axial water ligands from $Cr_2(O_2CH)_4$ using CI calculations on RHF orbitals.[6] Again if one assumes that the electron diffraction value is correct, axial water ligands lengthen the metal–metal bond of dichromium tetraacetate by 0.396 Å.

We see that many of the calculations done so far still disagree with experiment. In principle this disagreement could be settled by a large enough basis set and CI expansion, but we estimate that without empirical corrections the size of the necessary computation would be prohibitive today. A second approach is to employ smaller basis sets and limited CI and concentrate on trends for a series of related complexes. This approach assumes that errors due to limited basis set and limited electron correlation remain constant for closely related complexes. If the computational method consistently accounts for the physics of the problem, accurate trends should be calculated.

We have chosen the second approach for this study. We have undertaken to systematically extend and improve the computational studies on these complexes to achieve the goals of calculating accurate trends in Cr–Cr bond lengths and explaining these trends. Previous theoretical determinations of Cr–Cr bond length have not been complete optimizations; the geometry of the bridging ligands have either been unmodified[3] or in some cases modified according to available experimental data.[6] Our preliminary results have indicated that the geometry of the bridging ligand should have substantial effect upon the calculated Cr–Cr distance. We have sought to improve upon previous calculations by optimizing both the Cr–Cr bond and the bridging ligand geometry.

Theory

A computational difficulty is encountered when complexes with less than D_{4h} symmetry are studied. In RHF calculations on complexes of symmetry lower than D_{4h}, metal–metal bonds localize onto opposite Cr atoms. For example, in D_{2d} symmetry, the π_x bond will localize onto one metal, and the π_y onto the other, while the δ and σ bonds remain delocalized. Localization is energetically favorable at the Hartree–Fock level because it reduces the electron repulsion energy. CI calculations begun from RHF starting orbitals will delocalize the π electrons, but both Benard,[6] who did CI on RHF starting orbitals, and Hall,[2] using CI on generalized molecular orbital GMO starting orbitals, found that the results of calculations on $Cr_2(O_2CH)_4$ depend on whether the reference wave function is localized or delocalized. Benard found a shorter Cr–Cr distance when he used a localized reference configuration. Thus, one cannot compare calculations on complexes of different symmetry unless the theoretical method used gives the same results starting from localized or delocalized reference wave functions.

In this study we have used the generalized valence bond (GVB) method. The GVB method is a multiconfigurational self-consistent field calculation developed by Goddard.[35] For our system each GVB pair consisted of a metal–metal bonding orbital and its antibonding counterpart. An advantage of the GVB method is that it gives a properly delocalized solution for $Cr_2(O_2CH)_4$ even if the RHF starting orbitals are from a symmetry broken, localized solution. This was determined by perturbing the geometry of $Cr_2(O_2CH)_4$ slightly to lower the symmetry to D_{2d}, which allows the d–π orbitals to localized onto the metal

---

(31) Goodgame, M. M.; Goddard, W. A. *Phys. Rev. Lett.* **1982**, *48*, 135.

(32) Goodgame, M. M.; Goddard, W. A. *J. Phys. Chem.* **1981**, *85*, 3914.

(33) Walch, S. P.; Bauschlicher, C. W.; Roos, B. O.; Nelin, C. J. *J. Chem. Phys.* **1983**, *103*, 175.

(34) Kant, A.; Straus, B. *J. Chem. Phys.* **1966**, *45*, 3161.

(35) Bobrowicz, F. W.; Goddard, W. A. In *Methods of Electron Structure Theory*; Schaefer, H. F., Ed.; Plenum: New York, 1977.

Table I. Optimized Geometries (in Å and deg) of Free Bridging Ligands as a Function of Basis Set Splitting for 2s and 2p of C, N, and O

variables	STO-3G	split 2p	split 2s, 2p
	Formate		
CH	1.154	1.115	1.116
CO	1.352	1.273	1.253
OCO	129.6	130.6	131.0
O··O	2.447	2.314	2.280
	Amidate		
CH	1.146	1.111	1.115
CO	1.353	1.279	1.263
CN	1.404	1.329	1.305
NH	1.044	1.024	1.022
N··O	2.475	2.356	2.323
OCN	127.8	129.1	129.5
CNH	105.1	109.3	109.2
	Amidinate		
CH	1.136	1.106	1.109
CN	1.404	1.337	1.316
NH	1.043	1.023	1.021
N··N	2.499	2.393	2.363
NCN	125.6	126.9	127.8
CNH	104.8	109.3	108.6

atoms. These localized orbitals were then used to start a GVB calculation. The GVB self-consistent field (SCF) cycling yielded the same delocalized orbitals and CI coefficients as those obtained from delocalized starting orbitals. The GVB calculations mix the bonding and antibonding metal–metal bond orbitals very efficiently and therefore delocalize the metal–metal bonds even when starting from localized d orbitals. Thus, the GVB method may be used to compare systems of different symmetry.

For all calculations the basis sets were derived from that of Huzinaga.[36] The basis set on Cr is the modification of Huzinaga's (432-32-3) basis due to Williamson and Hall,[37] where a diffuse d and p orbital have been added to produce a "double-ζ" basis. The basis sets on C, N, and O are Huzinaga's (33-3) bases with the p function split to give (33-21). The basis set on H was Huzinaga's contraction of three primitive gaussians. Since the calculated Cr–Cr distance is dependent upon the bridging ligand geometry, the ligand basis set was carefully chosen to give consistent results for the three bridging ligands O_2CH, (NH)OCH, and $(NH)_2CH$. The geometry of the free ligands were optimized by using several contraction schemes for Huzinaga's (33-3) bases on C, N, and O. The results are shown in Table I. The largest basis set, (321-21) on C, N, and O, would have been too costly to use in the full complex, but it did serve as a standard for the free ligand optimizations. By splitting the p function on C, N, and O to give a (33-21) basis, we obtained geometries within 2% of those obtained with the (321-21) bases for all three bridging ligands. This is a modest basis set, especially for geometry optimizations. We do not, therefore, attempt to draw conclusions from the absolute values of our calculated bond parameters. Rather, we depend on calculating these parameters for a series of complexes and drawing conclusions from the more trustworthy trends in geometry.

Geometry optimizations were done by using analytical gradient techniques. The optimizations were said to be converged when the maximum gradient was less than 0.0075 Hartree/au or radians, and the average gradient was less than 0.005 Hartree/au or radians. When the above gradient criteria were met, the maximum stepsize were never greater than 0.001 au or radians.

Error Analysis. Since the criteria for convergence are small but nonzero values, some uncertainty in the calculated value of the Cr–Cr distance is unavoidable. The uncertainty can be divided into a part due to the nonzero gradient for the Cr–Cr bond itself and a part due to the uncertainty in the bridging ligand parameters. The uncertainty due to allowing a maximum gradient of ±0.0075 for the Cr–Cr bond was 0.05 Å for $Cr_2(O_2CH)_4$. Since this error was unacceptable, we calculated two Cr–Cr bond lengths for the formato complex, one that had a gradient between 0.00 and 0.0075 Hartree/au, and one that had a gradient between 0.00 and −0.0075 Hartree/au. We determined by interpolation that a Cr–Cr bond with a gradient of 0.001 Hartree/au has an uncertainty of less than 0.005 Å. We therefore required that the Cr–Cr gradient either be less than 0.001 or that two points that have gradients within the convergence limit be calculated and an interpolated value obtained. The uncertainty due to variations in the bridging ligand geometry was tested for $Cr_2(O_2CH)_4$ by optimizing the Cr–Cr distance with fixed bridging ligand parameters obtained from the 2.45 and 2.55 points of the potential curve. In both cases the optimal Cr–Cr distance was 2.490 ± 0.005 Å. Thus, the final results have an uncertainty of ±0.01 Å in the calculated Cr–Cr bonds.

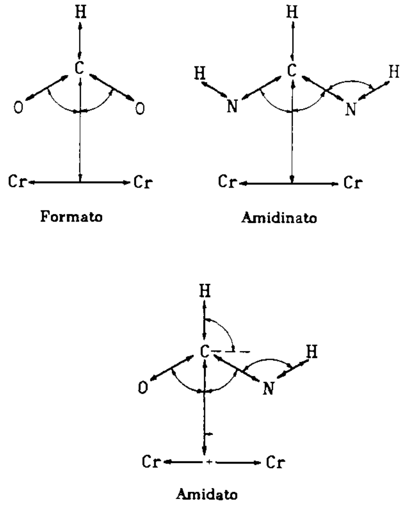

Figure 2. The variable schemes which were used for complete optimization of complexes without axial ligands are shown. Due to the lower (D_{2d}) symmetry the amidato complex has the extra variables of shift and tilt.

For $Cr_2(O_2CH)_4$ and $Cr_2((NH)_2CH)_4$ potential energy curves were calculated by allowing optimization of all variables except the Cr–Cr distance. Once the curves had been calculated, all variables were optimized simultaneously, starting from the point closest to the minimum of the potential curve. For $Cr_2((NH)_2CH)_4$ the gradient for the Cr–Cr bond at 2.30 Å was well below the convergence limit; therefore, the bond parameters at Cr–Cr = 2.30 Å represent the optimal geometry.

The calculated geometries of the axially ligated complexes, $Cr_2(O_2CH)_4(OH_2)_2$ and $Cr_2((NH)_2CH)_4(OH_2)_2$, are given in Table III. These calculations are not, however, complete geometry optimizations. The Cr–Cr and C to bond axis distances and the LCL (L = N, O) and CNH bond angles were optimized. The C–H bonds and the C–N bond were fixed, but their gradients were evaluated at the final geometry and were below the convergence criterion for maximum gradient. The C–O bond was fixed, because it was nearly constant at 1.275 (±0.001) Å over the range of Cr–Cr bond lengths 2.25 Å to 2.65 Å in $Cr_2(O_2CH)_4$. The O–H bond length and HOH angle of the axial water ligands were also fixed, because these variables should not directly affect the Cr–Cr bond.

All calculations were performed with the GAMESS program package.[38] Calculations were carried out on the Texas A&M University Amdahl 5850 computer, the Cornell National Supercomputer Facility FPS 264 processors, and a Cray X-MP supercomputer located by Cray Research, Mendota Heights, MN.

Results

Separating the individual interactions in a complete system is a difficult but important task. Initially we evaluated the response of the metal–metal bond to the O··O or N··N distance (the "bridge span" of the bridging ligand). The bridge span was changed by opening or closing the OCO or NCN angles, at constant C–O or C–N distance. At fixed spans, the C to metal–metal bond axis distances (see Figure 2) and Cr–Cr distances were optimized. The CNH angle in the amidinato complex, which influences the nitrogen hybrid orbital directed toward the Cr, was also optimized. The results of these calculations are shown in Figure 3. The Cr–Cr distance was calculated to be strongly dependent upon the L··L distance (L = N, O). In these calculations the Cr-bridge interaction is strong enough to set the Cr–Cr distance.

The results of the preliminary fixed ligand studies showed the necessity of complete geometry optimization for a systematic study

---

(36) *Gaussian Basis Sets for Molecular Calculations*; Huzinaga, S., Ed.; Elsevier: Amsterdam, 1984.

(37) Williamson, R. L.; Hall, M. B. *Int. J. Quantum Chem. Symp.* **1987**, *21*, 502.

(38) Guest, M. F.; S.E.R.C. Daresbury Laboratory, Warrington, WA4 4AD U.K.

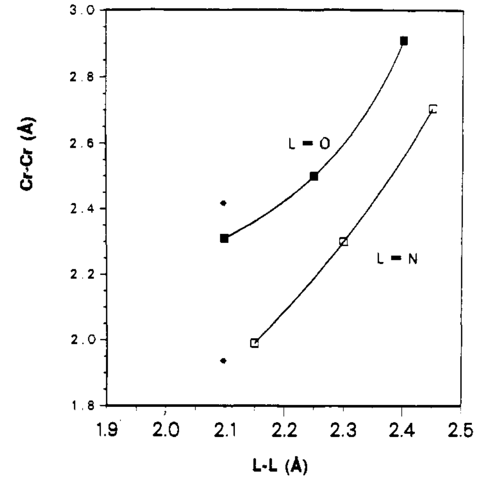

Figure 3. Response of Cr–Cr bond lengths to change in the ligand bridge span. The points indicated by (*) are from the study of Kok and Hall (ref 4).

Table II. Optimal Bond Lengths and Angles (in Å and deg) for Complexes without Axial Ligands

	calculation	experiment
	Tetracarboxylato[a]	
Cr–Cr	2.49 (1)	1.966 (14)
Cr–O	1.967	2.014 (8)
C–O	1.275	1.267 (5)
OCO	123.4	128.5 (3)
O··O	2.246	2.282 (12)
	Tetraamidato[b]	
Cr–Cr	2.38 (1)	1.937 (2)
Cr–O	1.953	1.959 (5)
Cr–N	2.040	2.080 (7)
off-center[c]	0.08	0.1 (1)[e]
tilt angle[c]	4.2	3.3 (9)[e]
C–O	1.292	1.29 (2)[e]
C–N	1.297	1.31 (5)[e]
OCN	123.3	121.6 (8)[e]
CNR	115.8	121.3 (7)[e]
O··N	2.278	2.27 (2)[e]
	Tetraamidinato[d]	
Cr–Cr	2.30	1.843 (2)
Cr–N	2.039	2.025 (5)
C–N	1.314	1.33 (1)[e]
NCN	122.8	116.3 (5)
N··N	2.307	2.27 (1)[e]

[a] Experimental complex is tetraacetate (ref 29). [b] Experimental bridging ligand is (2-xylylN)OCMe (ref 26). [c] The ligand moves and tilts toward the oxygen atom. [d] Experimental bridging ligand is $(NMe)_2CPh$ (ref 39). [e] Values are averages and standard deviations of crystallographically independent parameters.

of Cr–Cr bond lengths in these complexes. Geometry optimizations insure that the theory and not a prechosen geometrical parameter, such as the OCO angle, is controlling the Cr–Cr bond distance. The fully optimized geometries of the complexes without axial ligands are given in Table II, and the potential curves for the Cr–Cr bonds in $Cr_2(O_2CH)_4$ and $Cr_2((NH)_2CH)_4$ are shown in Figure 4. The $Cr_2((NH)OCH)_4$ complex, due to its lower symmetry (D_{2d}), has three more variables, as shown in Figure 2. The potential curve for this complex was first calculated with the line drawn through the CH bond constrained to be the perpendicular bisector of the Cr–Cr bond. The bridging ligand could not slide or tilt. When all variables were optimized we found that including the tilt and slide decreased the energy and moved the optimum Cr–Cr bond length from 2.40 to 2.38 Å. Table III shows the optimized geometries for the axially hydrated complexes $Cr_2(O_2CH)_4(OH_2)_2$ and $Cr_2((NH)_2CH)_4(OH_2)_2$.

As expected from previous calculations, the calculated Cr–Cr bond lengths are too long in every case. The intraligand bond parameters generally are in good agreement with experimental values. Some difference between the calculated and experimental intraligand parameters is expected for the amidato (R'C(NR)O) and amidinato (R'C(NR)$_2$ because of the difference between the model and experimental R and R' groups. The Cr–N and Cr–O bond lengths agree remarkably well with experiment, considering the moderate basis set size.

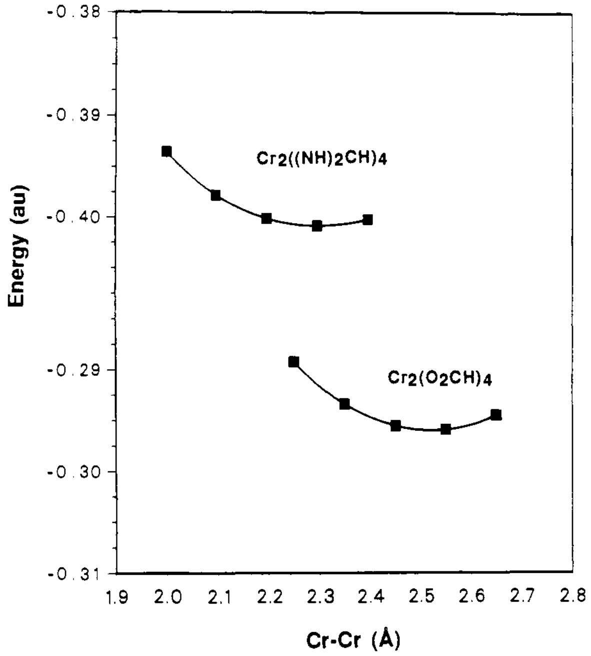

Figure 4. Potential energy curves for the chromium–chromium bond in dichromium tetraformate and dichromium tetraammidinate. For the true energy scales add −2832 au for tetraformate and −2674 au for ammidinate complex.

Table III. Calculated Bond Lengths and Angles (in Å and deg) for Axially Hydrated Complexes

	calculated	experimental[a]
	Tetracarboxylato	
Cr–Cr	2.60	2.362 (1)
Cr–O(bridge)	1.989	2.018 (8)
Cr–O(axial)	2.153	2.272 (3)
C–O	1.275[b]	1.265 (5)
OCO	124.3	123.1 (3)
O··O	2.254	2.224 (2)
	Tetraamidinato	
Cr–Cr	2.48	
Cr–O	2.346	
Cr–N	2.057	
C–N	1.314	
N··N	2.327	
NCN	123.7	
CNH	114.2	

[a] Experimental complex is $Cr_2(O_2CMe)_4(H_2O)$ (ref 24). [b] This distance is fixed from unhydrated complex.

Discussion

The large experimental variability of the Cr–Cr bond lengths of these complexes is evidence of a shallow potential well. The shallowness of the well makes the Cr–Cr bond sensitive to small perturbations, which in turn makes analysis of the Cr–Cr bonding difficult. The calculated potential curve is also very shallow, and calculated Cr–Cr bonds are longer than experiment in all cases. This does not necessarily mean that the wave function is especially poor but that the wave function would have to be extremely good to get the correct Cr–Cr bond distance. For our GVB calculations on the tetraformate complex a Cr–Cr bond length of 2.25 Å is only 4 kcal higher in energy than a Cr–Cr bond of 2.55 Å. Our calculations do give reasonable and consistent trends in Cr–Cr

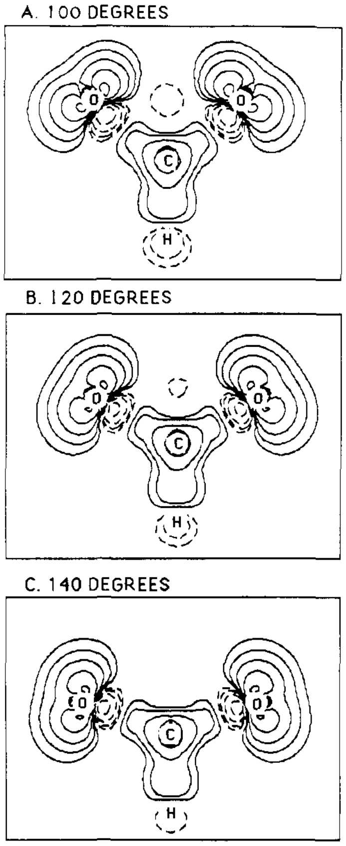
A. 100 DEGREES

B. 120 DEGREES

C. 140 DEGREES

Figure 5. Movement of oxygen lone pair as OCO angle is opened as shown by deformation density plots. The plots are obtained by subtracting spherical atoms and are contoured geometrically. Adjacent lines differ by a factor of 2, and the lowest contour is 0.0156 electrons/au^3.

Table IV. Mulliken and Lowdin Population Analysis and Core Orbital Energies for Cr Atoms with Various Bridging Ligands

	tetraformato	tetraamidinato
Mulliken	22.843	22.457
Lowdin	24.175	24.268
1s energy (au)	-220.652	-220.546
2s energy (au)	-26.743	-26.638

Table V. GVB Wave Function Properties for Axially Ligated Complexes at Cr–Cr = 2.50 Å

	tetraformato	tetraamidinato
	Energy (au)	
σ	-0.568	-0.416
σ^*	-0.226	-0.183
π	-0.493	-0.380
π^*	-0.379	-0.289
δ	-0.481	-0.360
δ^*	-0.403	-0.286
	Occupation	
σ	1.57	1.56
σ^*	0.43	0.44
π	1.18	1.20
π^*	0.82	0.80
δ	1.12	1.17
δ^*	0.88	0.83
	Pair Overlap	
σ	0.310	0.304
π	0.092	0.099
δ	0.060	0.085

bond distance for changes in the bridging ligands and the addition of axial ligands. The wave functions of the various complexes should therefore show the underlying causes of the observed trends.

We will begin by examining the calculated dependence of Cr–Cr bond upon axial and bridging ligands. We will analyze changes in both the geometries and the wave functions of the complexes as the bridging ligands are modified and axial ligands are added. The results of our calculations will then be compared to experiment, and finally to the results of previous calculations, in order to obtain a fuller understanding of the Cr–Cr bond in these complexes.

GVB Geometries and Wave Functions. Our initial studies showed the necessity of full geometry optimizations for complexes without axial ligands. The calculated Cr–N and Cr–O bonds are much stronger than the calculated Cr–Cr bond. If the span of the bridging ligand increases, the chromium atoms simply follow the bridging atoms out, with only a small change in Cr–N and Cr–O bond lengths. There is actually an amplification effect; the slopes of the lines in Figure 3 increase as the bridge spans increase. This is due to a rehybridization of the bridging ligand which forces the lone pair to point outward as the LCL angle opens. The change in the lone pair direction can be seen in Figure 5, which shows the calculated deformation density of the formato ligand at various OCO angles.

The calculated geometries of O_2CH and $(NH)_2CH$ change only slightly from point to point along the potential curve of the Cr–Cr bond. These slight adjustments keep the Cr–N and Cr–O distances nearly constant, and, although they are small, they are important for the accurate calculation of a potential curve as shallow as that of the Cr–Cr bond. Optimization of the bridging ligands is even more important when one compares the Cr–Cr bond lengths for different model bridging ligands, because the lines L = N and L = O of Figure 3 differ in slope and curvature. If we extrapolate the lines in Figure 3 to 2.10 Å, we see that the previous results of Kok and Hall are consistent with the present calculations. Kok and Hall overestimated the response of Cr–Cr distance to the change in the bridging ligands in large partly because they fixed the bridge span of both model ligands at 2.10 Å.

Our calculations show a steady decrease in the Cr–Cr bond length as the basicity of the bridging ligand increases. This is consistent with earlier theoretical studies of Benard,[6] Atha et al.,[12] and Kok and Hall.[3,4] One expects increased donation of electrons to the chromium as the basicity of the bridging ligand increases. The increased donation decreases the charge on the metal, weakens the electrostatic repulsion, and shortens the metal–metal bond. One would also expect expansions of the metal d-orbitals as the charge on the metal decreases, which would result in better d–d overlap and a stronger bond.

We can examine the wave function and its properties to see if these expectations are born out. The Mulliken and Lowdin population analyses, shown for a common Cr–Cr distance in Table IV, conflict; therefore, another method of evaluating the charge on the metal must be used. One can roughly compare the charge on an atom in different environments by noting the changes in core orbital energy levels. Higher energies indicate a lower potential at the Cr nucleus, which implies the presence of more electron density. Each Cr atom would thus experience a weaker repulsion from the other Cr nucleus. From the core orbital energies in Table IV we can infer that the sequence in metal charges for the complexes is formato > amidato > amidinato, which is consistent with metal–metal bond length change and the basicity of the ligand. Atha et al. reached a similar conclusion based on a combined theoretical and gas-phase X-ray photoelectron spectroscopy study of dichromium and dimolybdenum complexes.[12]

The GVB parameters given in Tables V and VI indicate the degree of similarity of the Cr–Cr σ, π, and δ bonds to typical covalent bonds. For a typical covalent bond, such as the one in H_2, one would calculate a large energy gap between the bonding and antibonding orbital, a bonding orbital occupation of nearly two electrons, and a large GVB pair overlap. The stronger Cr–Cr bonds more closely resemble typical covalent bonds; thus, we see that for all cases the σ bond is much stronger than the π or δ. The relative strength of the σ bond is not surprising, but the similarity of the π and δ bonds is surprising. The relative weakness

Table VI. GVB Wave Function Parameters for σ, π, and δ Bonds of Complexes without Axial Ligands at Cr–Cr = 2.40 Å

	tetraformato	tetraamidato[a]	tetraamidinato
		Energy (au)	
σ	−0.716	−0.621	−0.547
σ^*	−0.253	−0.229	−0.217
π	−0.601	−0.530	−0.481
π^*	−0.411	−0.369	−0.331
δ	−0.555	−0.486	−0.433
δ^*	−0.451	−0.392	−0.345
		Occupation	
σ	1.58	1.58	1.56
σ^*	0.42	0.42	0.44
π	1.23	1.23	1.25
π^*	0.77	0.77	0.75
δ	1.13	1.14	1.16
δ^*	0.87	0.86	0.84
		Pair Overlap	
σ	0.3211	0.3191	0.3076
π	0.1055	0.1178	0.1252
δ	0.0660	0.0717	0.0792

[a] The calculation at 2.40 Å for the tetraamidato complex was constrained such that a line through the C–H bond would be a perpendicular bisector of the Cr–Cr bond.

of the π and δ bonds is, however, consistent with the large change in Cr–Cr bond length upon axial ligation found experimentally for $Cr_2((NR)OCMe)_4$ (R = 2-xylyl). If each π bond were nearly as strong as the σ bond, then one would expect that axial ligation by predominantly σ donors such as H_2O and THF would directly weaken only the σ bond and therefore have a small effect on the Cr–Cr distance. Another surprising feature is that the σ bond weakens as the bridging ligand goes from formato to amidinato. This can be seen by the larger energy gap between σ and σ^* and the larger GVB overlap for the formato complex. The σ and σ^* orbitals of the formato complex have greater contributions from the diffuse 4s, and the resulting increase in overlap stabilizes the σ orbital and destabilizes the σ^*. Bursten and Clark, using X-a calculations, note that involvement of the 4s orbital will stabilize the Cr–Cr bond, but they found essentially no involvement of the 4s orbital in the Cr–Cr σ bond.[40] We find, however, a small but significant 4s involvement in the σ and σ^* orbitals of the formato complex. The 4s involvement in the σ bond is less for the amidato complex and smallest for the amidinato complex.

When we add axial water ligands, the Cr–Cr bond lengthens by 0.11 Å for the formato complex and 0.18 Å for the amidinato complex. Thus, in our calculations the amidinato complex is almost twice as sensitive to axial ligation as the formato complex despite the shorter Cr–O(ax) bond and greater change in the GVB parameters for the σ bond of the formato complex. Donation by axial ligands will have two competing effects on the Cr–Cr bond length. Donation to the metal decreases the charge on the Cr atoms and therefore weakens their electrostatic repulsion. The axial donation, however, weakens the Cr–Cr σ bond, because donation is primarily into a σ^* orbital. For each complex we can estimate the magnitude of charge reduction by the change in core energies and the weakening of the σ bond by the changes in its GVB parameters, which are given in Table VII. We can then account for the relative sensitivity of the tetraformato and tetraamidinato complexes to axial ligation by the balance of these effects.

The Cr–O(ax) bond in the formato complex is shorter and presumably stronger than that of the amidinato complex and therefore causes a greater change in the GVB parameters of the Cr–Cr σ bond. Thus, we see in Table VII that the σ bond parameters of the formato complex change more than those of the amidinato complex. The charge on the Cr atoms, however, decreases more for the formato complex than for the amidinato complex. This is shown by the greater increase in the Cr core orbital potentials for the formato complex. The lower initial charge on the Cr atoms of the amidinato complex contributes to the shorter bond in the absence of axial ligands, but it also makes the bond more responsive to addition of axial ligands, because the lengthening effect of donation into the σ^* orbital is not offset by decreasing charge on the metal. The formato complex has a long Cr–Cr bond in the absence of axial ligands due, in part, to the greater charge on the Cr atoms. The greater charge on the Cr atoms, however, along with the lower energy of the σ^* level, favors greater charge transfer from the axial ligands to the metal. The lengthening of the Cr–Cr bond upon axial ligation is, therefore, mitigated in the tetraformate complex by the counter effect of decreased charge on the Cr atom.

Table VII. Changes in Core Orbital Energies and GVB Parameters upon Axial Ligation

	tetraformato	tetraamidinato
ΔE 1s (au)	0.073	0.056
ΔE 2s (au)	0.073	0.056
change in σ/σ^* gap (au)	−0.122	−0.097
change in GVB σ bond overlap	−0.019	−0.004

From another point of view, the presence of axial ligands lessens the difference between the Cr–Cr bond length of the tetraformate complex and the tetraamidinate complex. The electrons donated from the axial ligands decrease the importance of donation from the bridging ligands in setting the Cr–Cr bond distance. The weaker donation by the formato ligand, relative to the amidinato ligand, results in greater donation by the axial ligands. The changes in Cr–Cr bond length upon changing bridging and axial ligation are interdependent. The change in bond length upon axial ligation found for complexes with noncarboxylate bridging ligands will differ from that of the carboxylate complexes.

In addition to the effects described above, Benard[6] attributes the lengthening of Cr–Cr bonds upon axial ligation to the narrowing of the σ–σ^* gap, which results in a larger CI coefficient for configurations containing σ^* character. We find, however, very little effect on the GVB coefficients of the σ bond. Addition of more basic axial ligands, such as pyridine, might have greater effect on the CI coefficients.

Comparison with Experiment for Complexes without Axial Ligands. The sensitivity of the Cr–Cr bond to changes in ligation and the necessity of using model complexes for calculations make comparisons with experiment difficult. Crystallographic data are available for two amidato complexes of the general formula $Cr_2((N\text{-aryl})OCMe)_4$ which show quite different Cr–Cr distances. For aryl = phenyl, Cr–Cr = 1.873 (4) Å, for aryl = 2-xylyl, Cr–Cr = 1.937 (2) Å.[26] Cotton postulates that the Cr–Cr bond lengthens for aryl = 2-xylyl because the 2-xylyl ring twists out of the NCO plane, reducing the conjugation of the aryl π orbitals with the NCO π system.[26] Thus aryl = 2-xylyl is the more appropriate comparison with the model N–H, which of course has no extended conjugation. For the amidinato complex we compare our results to the experimental structure for $Cr_2((NMe)_2CPh)_4$ (Cr–Cr = 1.843 (4) Å.[39]

One should note that the uncertainties given for the experimental results in Tables II and III do not always represent the statistical factors derived from the X-ray diffraction experiment. For some cases, especially the tetraamidato complex, bonds which are equivalent in our calculations are inequivalent in the space group of the crystal. In these cases we average the inequivalent values and report this average and standard deviation. For example, all four C–N bonds in $Cr_2((NH)OCH)_4$ are equivalent by symmetry in our calculation. In the X-ray structure of $Cr_2((2\text{-xylylNOCMe})_4$, however, the four C–N bonds have a remarkable 0.1 Å range; therefore, we have averaged these four values and list this average and standard deviation, along with an appropriate footnote.

Our calculated order of Cr–Cr distance for the series of complexes of the type $Cr_2(O_2CH)_4$, $Cr_2((NH)OCH)_4$, $Cr_2((NH)_2CH)_4$ are in agreement with experiment. In Table VIII the calculated change in Cr–Cr distance is compared to experimental

---

(39) Bino, A.; Cotton, F. A.; Kaim, W. *Inorg. Chem.* **1979**, *18*, 3566.
(40) Bursten, B. E.; Clark, D. L. *Polyhedron* **1987**, *6*, 695.

Table VIII. Experimental and Calculated Changes in Cr–Cr Bond Lengths (Å) for $Cr_2(bridge)_4$ Complexes[a]

	calculated	experimental
$RC(NR^1)_2$ to $R^2CO(NR^3)$	0.08	0.094
$R^2CO(NR^3)$ to HCO_2	0.11 (0.61)[b]	0.029[c]
$RC(NR^1)_2$ to HCO_2	0.19 (0.48)[d]	0.123[c]

[a] For calculated results R = R^1 = R^2 = R^3 = H. For experimental results R = phenyl; R^1 = R^2 = Me; R^3 = 2-xylyl (ref 26 and 39). [b] Reference 6. [c] Experimental data for the formato ligand is from electron diffraction on the acetato ligand (ref 29). [d] Reference 3.

values for the sequence of bridging ligands $RC(NR^1)_2$, $R^2CO(NR^3)$, R^4CO_2. The geometries of the bridging ligands, and the Cr-bridge bond parameters in general show good agreement between calculation and experiment. However, a close comparison of the calculated geometry parameters for $Cr_2(O_2CH)_4$ and the geometry found by electron diffraction for $Cr_2(O_2CMe)_4$ (given in Table II) reveals some unusual differences. The OCO angle found by electron diffraction is 5.0° greater than either calculation or X-ray diffraction of the hydrated acetato or formato complexes. Our calculations show a weak dependence of this angle on the Cr–Cr distance, and it is surprising that the angle *opens* as the Cr atoms move in by 0.4 Å.

The electron diffraction experiment also predicts a stronger Cr–Cr bond than one would expect from theory; it yields a force constant for the Cr–Cr bond which is four times that of the Cr–O bond. The force constant of 3.8 mdyn/Å for the Cr–Cr bond obtained by electron diffraction is surprising if one considers that the Cr–Cr stretching frequency in the $^1\Sigma_g$ state of the bare dimer is 427.5 cm^{-1} which gives a force constant of 2.80 (mdyn/Å).[41] If the numbers given by Fink are correct, it would indicate that the bond of the complex is both longer, and stronger, than the bond of the bare dimer (for which d_{Cr-Cr} = 1.68 Å) in disagreement with Badger's rule. Badger's rule indicates an inverse relation between bond length and force constant.[42]

On the basis of the above considerations, we believe the Cr–Cr bond length found by electron diffraction to be questionable. The refinement of the structure depends upon both the force constant and the length of a bond, and we feel that an incorrect estimate of the force constant has contributed to an error in the Cr–Cr bond length. We propose that the change in Cr–Cr distance from the amidato complex to acetato complex to acetato should be closer to 0.1 Å, thus for the acetato complex we estimate a Cr–Cr bond of 2.05–2.10 Å, 0.10–0.15 Å longer than the electron diffraction result.

Comparison with Experiment for Complexes with Axial Ligands. The paucity of complexes which have been characterized both with and without axial ligands make comparisons of calculated and experimental changes in Cr–Cr bond length upon axial ligation difficult. Only $Cr_2((NR)OCMe)_4$ (R = 2-xylyl) has been characterized with and without axial ligands by X-ray crystallography. This complex, however, was characterized with axial THF and pyridine but not H_2O ligands. The calculations also underestimate the effect of axial ligation; the change in Cr–Cr bond length upon axial ligation which is obtained by interpolation for the amidato complex is only half the response obtained experimentally for THF ligands. Even at a level of theory which is adequate for determining the structure of most transition-metal complexes, the strength of the Cr–Cr bond is underestimated, because the calculated Cr–Cr bond is long and weak without axial ligands and does not undergo the radical change in length which is seen experimentally upon the addition of axial ligands. The calculations do, however, show trends in the response of Cr–Cr bonds to axial ligation. These trends depend upon the nature and relative strength of the calculated Cr–Cr bond, and we may compare these trends to experimental results.

Table IX. Predicted Values of Cr–Cr Bond Lengths upon Removal of Axial Ligands from $Cr_2(O_2CR)_4L_2$ Complexes (in Å)

R	L	d_{Cr-Cr} (Å)	d_{Cr-L} (Å)	predicted d_{Cr-Cr}
H[a]	Pyr	2.41	2.31	2.09
Me[b]	Pyr	2.37	2.34	2.05
2-phenyl-Ph[c]	THF	2.32	2.28	2.10
$C(Ph)_3$[d]	Et_2O	2.30	2.30	2.08

[a] Reference 21. [b] Reference 23. [c] Reference 27. [d] Reference 28.

The previously mentioned experiments of Cotton and Wang[19] showed that the relatively long and weak Cr–Cr bonds of the complexes they studied were more sensitive to changes in bridging ligand pK_a than axial ligand pK_a (slopes of −0.04 and 0.008 Å/(pK_a unit), respectively). The complexes with "super-short" Cr–Cr bonds, however, are relatively insensitive to changes in bridging ligands and have a total range of metal–metal bond lengths of about 0.11 Å.[20] The relative sensitivity of the metal-metal bond to bridging and axial ligation, ΔCr–Cr(bridge)/ΔCr–Cr(ax), increases as the Cr–Cr bond lengthens. Our calculations show the same trend. Upon axial hydration the Cr–Cr bond lengthens by 0.18 Å for $Cr_2((NH)_2CH)_4$ and 0.11 Å for $Cr_2(O_2CH)_4$. If we assume that the response of the $Cr_2((NH)OCH)_4$ complex can be interpolated from the other two complexes, then the relative response to axial ligation for $Cr_2(O_2CH)_4$, $Cr_2((NH)OCH)_4$, and $Cr_2((NH)_2CH)_4$ should be roughly in the proportion 1.0:1.3:1.6, respectively.

We can compare the response of tetracarboxylato and tetraamidato complexes to axial ligation based on the experimental results for the amidato complex $Cr_2((NR)OCMe)_4$ (R = 2-xylyl) to determine if the 1.0:1.3 ratio gives consistent results for different axial ligands. The Cr–Cr bond lengthens by 0.417 and 0.284 Å upon addition of axial pyridine and THF ligands, respectively;[25] therefore, we estimate for tetracarboxylates a bond shortening of approximately 0.32 Å upon removal of axial pyridines and approximately 0.22 Å for axial THF ligands. Table IX shows the Cr–Cr bond lengths in some axially ligated tetracarboxylates, along with our predicted bond shortening. Unfortunately neither dichromium tetraformate nor tetraacetate have been characterized with axial THF ligands; however, the pK_a values for aqueous solutions of the bridging ligands used in comparison do not differ greatly from those of acetic acid and formic acid.[43] The predicted Cr–Cr bond length for all cases is 2.08 ± 0.03 Å. This is consistent with our prediction based on the response of the Cr–Cr bond to changes bridging ligands.

Comparison with Previous Calculations. Our results on the tetraformate complexes agree quite well with those of Benard,[6] who calculated Cr–Cr bond lengths of 2.58 and 2.53 Å for $Cr_2(O_2CH)_4$ and $Cr_2(O_2CH)_4(OH_2)_2$, respectively. There is a remarkable difference, however, between Benard's value of 1.92 Å and ours of 2.38 Å for the Cr–Cr distance in $Cr_2((NH)OCH)_4$. Our calculated geometry parameters for the bridging ligand do not differ from the experimental values that Benard uses by enough to account for this difference. The greater part of the Cr–Cr bond length difference must be due to differences in the approximate wave functions. We believe that the GVB calculation should provide consistent results for D_{4h} and D_{2d} symmetries and, perhaps, as noted in the Theory section, that the CI has not properly delocalized the Cr–Cr bond in Benard's calculation, and the bond is too short because it is still dominated by the localized RHF component of the wave function.

Some calculations do give short Cr–Cr bonds. Ziegler calculated a Cr–Cr bond length of 1.87 Å Hartree–Fock–Slater (HFS) calculations.[11] Thus, the HFS method predicts a shorter Cr–Cr bond than that obtained by electron diffraction. The bridging ligand geometry used in Ziegler's calculation was obtained from the gas-phase electron diffraction of Kektar and Fink, and "the metal–metal distance R_{MM} was varied under the constraint of fixed

---

[41] Diella, D. P.; Lipson, R. H.; Moskovits, M.; Taylor, K. *Resonance Raman Studies of Metal Dimers and Metal Clusters*; Proceedings of the 8th Raman Conference, Bordeaux, France, 1982.

[42] (a) Badger, R. M. *J. Chem. Phys.* **1934**, *2*, 128. (b) Badger, R. M. *J. Chem. Phys.* **1935**, *3*, 710.

[43] The pK_a of 2-phenylbenzoic acid is 3.46, that of triphenyl acetic is approximately 3.5 based on the series acetic = 4.74, phenyl acetic = 4.31, biphenyl acetic = 3.96, and that of formic acid is 3.75.

M–O distances, with the rest of the molecule rigid". Goddard has developed a modified GVB (M-GVB) program which uses empirical corrections for certain two-electron integrals, and by using this program he has calculated a short bond for Cr_2.[44] These systems are very difficult to describe theoretically, and experience has shown that an isolated calculation can get the "right" answer for the wrong reason. It would be useful to know how well these methods handle the well-studied trends, rather than isolated controversial cases.

Conclusion

GVB calculations do not provide correct absolute values for Cr–Cr bond length, but they do provide wave functions with the correct physical properties, which we may use to accurately predict trends. Therefore, we cannot predict a priori Cr–Cr bond lengths, but we can indicate responses of Cr–Cr bond lengths to changes in bridging ligation and relative responses to axial ligation. Our calculations indicate that the Cr–Cr bond length in anhydrous dichromium tetraacetate should be longer than either the amidato or amidinato complexes. Our calculations of the response of Cr–Cr bond length both to changes in the bridging ligands and relative changes in Cr–Cr bond length upon axial ligation are consistent with a Cr–Cr bond length of 2.05–2.10 Å for dichromium tetraacetate. We also conclude that the bridging and axial ligands do not effect the Cr–Cr bond length independently but cooperatively. Bridging ligands with lower electronegativity result in shorter Cr–Cr bonds, but they also make the change in bond length upon axial ligation greater.

Acknowledgment. We than the National Science Foundation (Grant No. CHE 86-19420) and the Robert A. Welch Foundation (Grant No. A-648) for support of this work. This research was conducted in part with use of the Cornell National Supercomputer Facility, a resource for the Center for Theory and Simulation in Science and Engineering at Cornell University, which is funded in part by the National Science Foundation, New York State, and the IBM corporation. We also gratefully acknowledge Cray Research, Mendota Heights, MN for a generous grant of computer time.

---

(44) Goodgame, M. M.; Goddard, W. A. *Phys. Rev. Lett.* **1985,** *54,* 661.

Noncatalyzed, Homogeneously Catalyzed, and Heterogeneously Catalyzed Formyl Formation

George Blyholder* and Michael Lawless

Contribution from the Department of Chemistry, University of Arkansas, Fayetteville, Arkansas 72701. *Received May 23, 1988*

Abstract: Potential energy surfaces have been calculated for H migration onto a carbonyl to give a formyl structure for a noncatalyzed, a homogeneously catalyzed, and a heterogeneously catalyzed reaction using a semiempirical MINDO procedure. For the $H_2 + CO$ reaction to give formaldehyde, the high activation energy is due to the fact that, in the limited orbital space available, the H–H bond must be almost entirely eliminated before the two H atoms are far enough apart to both form strong bonds with the carbon atom. For the homogeneous reaction $(CO)_4FeH^- \rightarrow (CO)_3FeCHO^-$ the activation energy is reduced to 44 kcal/mol because the H maintains bonding with the Fe while the C–H bond is forming, but the activation energy is still high because the highest occupied molecular orbital of the formyl product is an energetically unsuitable place to put electrons. In the heterogeneous process $HFe_{12}CO \rightarrow Fe_{12}CHO$, the activation energy is reduced to 5 kcal/mol because the H and C interaction with the large number of orbitals in the Fe sp band accommodates the changing H and C geometry and bonding with relatively little energy change. The consequences of this explicit comparison of homogeneous and heterogeneous catalysis are discussed.

The nature of the catalytic process has been a concern of chemists since chemistry became an experimental science. In 1836 Berzelius[1] brought together the known observations on enhanced chemcial activity, and to focus attention on the phenomena, he gave it a name, catalysis. For convenience he designated a causitive agent as the catalytic force but clearly indicated that the phenomena were rooted in the standard electrochemical affinities of matter. Current reaction rate theory (activated complexes on a potential energy surface) in conjunction with thermodynamics (the catalyst does not formally appear as a reactant or product and so cannot affect initial and final states, i.e. equilibrium) designates the role of the catalysts in enhancing a reaction rate as providing an alternative reaction path that has a lower activation energy.[2,3]

At the heart of catalysis, then, is the determination of potential energy surfaces (PES) for reactions and definition of those factors that cause different reaction channels to have different barrier heights. Ultimately, reactivity must be treated as a dynamic process, but it has been noted that the major limitation to the accuracy of all the classical, quantum, and statistical dynamics methods comes from the quality of the potential energy surface used. In this paper the fundamental nature of the catalytic process is probed by determining the PES for one reaction (the addition of hydrogen to the carbon atom of a carbonyl group) in two metal-catalyzed processes and in a noncatalyzed reaction.

Because catalysis is such a widely used and economically important industrial process, there is a great deal of practical empirical knowledge about catalytic reactions but relatively much less understanding of the mechanistic details of these catalytic reactions. As a starting point to a molecular understanding of metal-catalyzed reactions, an analogy between homogeneous and heterogeneous reactions often has been proposed.[4] The molecular orbital model for chemisorbed CO,[5,6] which has been highly

---

(1) Berzelius, J. J. *Ann. Chim. Phys.* **1836,** *61,* 146.

(2) Bond, G. C. *Heterogeneous Catalysis: Principles and Applications*, 2nd ed.; Clarendon Press: Oxford, 1987.

(3) Robertson, A. J. B. *Catalysis of Gas Reactions by Metals*; Logos Press: London, 1970.

(4) (a) *Catalysis: Heterogeneous and Homogeneous*; Proceedings of the International Symposium on the Relations between Heterogeneous and Homogeneous Catalytic Phenomena, Brussels, 1974; Delmon, B., Jannes, G.; Elsevier: Amsterdam, The Netherlands, 1975. (b) Muetterties, E. L. *Chem. Soc. Rev.* **1982,** *11,* 283. (c) Muetterties, E. L.; Burch, R. R.; Stolzenberg, A. M. *Annu. Rev. Phys. Chem.* **1982,** *33,* 89.

0002-7863/89/1511-1275$01.50/0 © 1989 American Chemical Society